ARTICLE

Generation of cell-laden hydrogel microspheres using 3D printing-enabled microfluidics

Sanika Suvarnapathaki,[b] Rafael Ramos,[b] Stephen W. Sawyer, Shannon McLoughlin, Andrew Ramos, Sarah Venn, and Pranav Soman[a]
Department of Biomedical and Chemical Engineering, Syracuse University, Syracuse, New York 13210, USA

(Received 31 January 2018; accepted 22 March 2018)

3D printing has been shown to be a robust and inexpensive manufacturing tool for a range of applications within biomedical science. Here we report the design and fabrication of a 3D printer-enabled microfluidic device used to generate cell-laden hydrogel microspheres of tunable sizes. An inverse mold was printed using a 3D printer, and replica molding was used to fabricate a PDMS microfluidic device. Intersecting channel geometry was used to generate perfluorodecalin oil-coated gelatin methacrylate (GelMA) microspheres of varying sizes (35–250 μm diameters). Process parameters such as viscosity profile and UV cross-linking times were determined for a range of GelMA concentrations (7–15% w/v). Empirical relationships between flow rates of GelMA and oil phases, microspheres size, and associated swelling properties were determined. For cell experiments, GelMA was mixed with human osteosarcoma Saos-2 cells, to generate cell-laden GelMA microspheres with high long-term viability. This simple, inexpensive method does not require the use of traditional cleanroom facilities and when combined with the appropriate flow setup is robust enough to yield tunable cell-laden hydrogel microspheres for potential tissue engineering applications.

I. INTRODUCTION

Over the past decade, different strategies have been pursued to develop cell-culture systems to understand fundamental cell–cell and cell–extracellular interaction in the third dimension (3D). Cell-laden microspheres using microfluidic technology has been widely used as model cell-culture platform as it integrates the extracellular-matrix mimicking properties of hydrogels with the miniaturization capability of microfluidics.[1–4] To incorporate cells within microspheres, living cells are dispersed in a biocompatible hydrogel and the micrometer scale of the spheres allows for sufficient nutrient to support high viability of encapsulated cells.[4–6] Biochemical and biophysical properties of the hydrogel can also be modulated to ensure ideal environment for short- and long-term 3D cell culture. As a result, cell-laden microspheres have used a variety of synthetic, semi-synthetic, and natural hydrogels that provide the necessary mechanical properties, cytocompatibility, and nutrient permeability for different cell types, and have been widely used as a reproducible high-throughput cost-effective platform in cell biology and biomedical engineering.

Conventional methods to fabricate hydrogel microspheres involve the emulsification of a prepolymer hydrogel solution within an immiscible continuous phase, followed by gelation of emulsion particles.[7,8] Gelation is performed using sonication; however, this results in polydisperse sphere sizes and damages the encapsulated cells. As a result, microfluidic flow-focusing devices have been used to generate monodisperse microspheres with tunable sizes for various biomedical applications.[9–11] In these devices, an intersecting channel geometry is created where a fluid (dispersed phase) from one channel is broken up into microspheres by shear stress generated using a flow of immiscible fluid (continuous phase) from the other channel. Presently, microfluidic devices to generate hydrogel microspheres are fabricated using soft lithographic techniques, but these methods are expensive, complicated, and require the use of expensive cleanroom facilities. An alternate and inexpensive fabrication method is the use of glass-capillary-based devices. However, this method is complex and requires skilled operators and specialized equipment such as pipette puller and a microforge.[12] 3D printing has gained interest and popularity in the recent years, as an inexpensive alternative to fabricate microfluidic devices as this method allows rapid prototyping from design to manufacturing within less than a day.[12–19]

In this work, we have used 3D printing to design and fabricate a negative mold that is used to assemble a PDMS microfluidic flow-focusing device. We report that gelatin methacrylate (GelMA) microspheres of different sizes (35–250 μm diameter) can be generated using the device. Relationships between flow rates of aqueous GelMA and oil phases, viscoelastic properties, microsphere size, UV

[a]Address all correspondence to this author.
e-mail: psoman@syr.edu
[b]These authors contributed equally to this work.
DOI: 10.1557/jmr.2018.77

cross-linking time, and associated swelling were obtained. Cell-laden GelMA microspheres with high and long-term cell viability were generated using this device. This method does not require the use of traditional cleanroom facilities, or specialized equipment, and is a simple, inexpensive method to generate monodispersed microspheres with high reliability for potential biomedical engineering applications.

II. EXPERIMENTAL DESIGN

A. Device fabrication

The device was fabricated using a 3D extrusion printing and replica casting-molding approach. Inventor (Autodesk, Inc., San Rafael, California) was used to design a negative mold with optimized dimensions, after which the structure was exported as an STL file. The design was printed from VeroClear plastic using an ObJet 30 Pro 3D extrusion printer (Stratasys Inc, Eden Prairie, Minnesota) at the Cornell Nanobiotechnology Center (NBTC) in Ithaca, NY. After printing, the mold was washed (3×) with an aqueous 30% (w/v) KOH solution to remove any excess polymer residue. The transition from an opaque to a transparent plastic indicated that the mold was ready to use. This master mold was used to cast PDMS at a 4:1 (w/w) base to curing agent ratio. The mixture was degassed and subsequently cured for 4 h at 60 °C, before carefully being cut from the mold. The solid silicone device was then plasma bonded (90 s, 10 psi oxygen pressure) face down to a clear glass slide of appropriate dimensions to create an air-tight seal.

B. Synthesis and characterization of GelMA

1. GelMA synthesis

GelMA was synthesized as previously described.[20,21] Briefly, 10 g of Type A porcine skin Gelatin (MilliPore Sigma, Bedford, Massachusetts) was dissolved into 100 mL of Dulbecco's phosphate buffered saline (DPBS; GIBCO) at 60 °C and stirred until fully dissolved. 8 mL of methacrylic anhydride (MA; MilliPore Sigma, Bedford, Massachusetts) were slowly added under stirring conditions. The mixture was then allowed to react for 3 h at 60 °C. Following a dilution of 100 mL of warm DPBS, the mixture was dialyzed against distilled water using 12–14 kDa cutoff dialysis tubing for 1 week at 50 °C. The solution was lyophilized for 1 week to generate a white porous foam and stored at −80 °C until further use. Prepolymer solutions were made by mixing freeze-dried GelMA macromers with varying amounts of distilled water to different solution concentrations (w/v). UV photoinitiator Igracure 2959 (Ciba Specialty Chemicals, Basel, Switzerland) was added to yield a final concentration of 0.5% (w/v).

2. Viscosity characterization

An AR-G2 rheometer (TA Instruments, New Castle, DE) was used to obtain the viscosity at high shear of prepolymer solutions of varying GelMa concentrations [3, 5, 6, 7, 8, 10, 12, and 15% (w/v)]. A parallel plate setup with a 40-mm-diameter steel geometry was used as the top plate, while a Peltier heating plate (522310.902 assembly) was defined as the bottom geometry to ensure that tests could be performed at 37 °C to replicate expected experimental conditions. 2 mL of each solution were used and a 1.5-mm gap was maintained. After equilibrating temperature for two minutes, the samples were subjected to a steady state flow procedure where shear rate was ramped from 0.1 to 1000 (1/s).

C. Generation of GelMA microspheres

Aqueous GelMA solution and fluorinated perfluorodecalin oil (Synquest Laboratories, Alachua, Florida) were selected as the dispersion and continuous phases, respectively.[22,23] A CorSolutions PneuWave dual channel pump (CorSolutions, Ithaca, New York), with a flow rate range of 0–120 μL/min for pressures from 0 to 14.5 psi, respectively, was used for this work. The pump was connected to the microfluidic device using FEP microtubing (ID: 0.020″; INDEX Health & Science Inc LLC, Oak Harbor, Washington) capped with 23G-1 needles. The aqueous GelMA phase consisted of a single tube, while the oil phase branched off through the use of a Y-junction to ensure a dual inlet with equal flow rates. GelMA solution was flown through a vertical channel of the chip, while the oil was flown through the horizontal side channels at both inlets. A heating fan (37 °C) was used to ensure that GelMA does not gel within the device. The two phases merged at the cross section of the T-junction in the chip, to form microspheres which were collected in the form of emulsions. GelMA microsphere emulsions were crosslinked using UV light (output power 850 mW, OmniCure S2000, Excelitas Technologies Corp., Waltham, Massachusetts). The swelling profile of microspheres was analyzed by placing them in DI water, and recording the change in the average diameter for a period of 4 h at 15-min intervals using an inverted bright-field microscope (Zeiss Axiovert 40 CFL with Phase Contrast; Carl Zeiss AG, Oberkochen, Germany).

All components of the experimental setup except for the pump were sterilized prior to every test. Fittings and connectors such as Luer Locks, Y-junctions, and Inlet/Outlet hoops were soaked in 100% cell-culture–grade ethanol and left to sit under UV-light overnight. Additional connective tubing along with the actual microfluidic chip was autoclaved. GelMA solutions were sterile filtered using a 0.20 μm filter (Corning Inc, Corning, New York) and the perfluorodecalin oil was autoclaved.

D. Generation of cell-laden GelMA

Human osteosarcoma cells (Saos-2; ATCC) were used as model cells for encapsulation experiments. Cells were cultured in T75 flasks (ThermoFisher Scientific, Waltham, Massachusetts) and maintained in DMEM media (Life Technologies, Carlsbad, California) with 10% fetal bovine serum (v/v) (Atlanta Biologics, Flowery Branch, Georgia), 1% penicillin-streptomycin (Life Technologies, Carlsbad, California), and 1% GlutamMAX (Life Technologies, Carlsbad, California). Cells were routinely passaged as per the manufacturer's protocol with 0.25% trypsin–EDTA (Life Technologies, Carlsbad, California) and stored at 37 °C with 5% CO_2.

Before cellular encapsulation, GelMA solutions were sterile filtered and stored at 2 °C in autoclaved Pyrex bottles (Corning Inc., Corning, New York) wrapped with tin foil. Saos-2 cell solutions were transferred into sterile GelMA solutions of varying densities. The mixed cell-GelMA solutions were flown through the vertical channel of the PDMS chip while the oil phase was flown through the horizontal channels to form microsphere emulsions. Cell-laden microspheres were collected and crosslinked using UV light and stored in DMEM media (Life Technologies, Carlsbad, California) in an incubator at 37 °C with 5% CO_2, and cell viability was analyzed at specific time points.

Cell viability was measured by fluorescently labeling with Calcein-AM (green-live) and ethidium homodimer-1 (red-dead) and then visualized with an inverted phase contrast microscope (Zeiss Axiovert, Carl Zeiss AG, Oberkochen, Germany).

E. Statistical analysis

One-way ANOVA and Bonferroni pair-wise tests were performed to compare cell viabilities between different time points. Also, Pearson's correlation coefficient was calculated to identify any correlation between encapsulated cell number and average microspheres size, with P-values <0.05 considered to be statistically significant.

III. RESULTS AND DISCUSSION

A. Device fabrication

ObJet 30 Pro 3D extrusion printer was used to print a negative mold in VeroClear plastic. The mold was designed with channel widths of 150 μm and channel height of 4 mm [Figs. 1(a) and 1(b)]. Rectangular chambers of XYZ dimensions 5.70 × 7.1 × 4 mm were created to facilitate easy integration with the connecting tubing. A mold rim of 5 mm was designed around the mold to prevent buckling during the subsequent PDMS casting process. The printing resolution of Veroclear ~16 μm was found to be sufficient for this work; however, alternate polymer blends such as RGD525, RGD430, and RGD450 can be used if higher resolution is desired. The mold was used to replicate cast PDMS devices that were subsequently bonded with glass substrate using plasma bonding. The 4:1 (w/w) mixing ratio for PDMS was found to be easy to peel off from the mold surface with high repeatability. The T-junction channel geometry facilitated the integration of the device with two independent flows, aqueous GelMA hydrogel solution, and hydrophobic oil solutions, and allows the formation of oil-coated GelMA microspheres that can be collected via a single outlet in the form of microsphere emulsions [Fig. 1(c)]. Collected emulsions were subsequently crosslinked with UV light [Figs. 1(d) and 1(e)].

GelMA was chosen as our model hydrogel to encapsulate cells as it is a collagen derivative, which possesses RGD groups necessary for cell adhesion, contains readily tunable mechanical properties, and exhibits high structural integrity for experiments lasting over one month.[20,21] Furthermore, GelMA is capable of being UV crosslinked with minimal negative side effects to the encapsulated cells and their properties have shown consistency between batches.[5,24–27]

B. Optimization of process parameters

1. Flow rates

To obtain a large size range for oil-coated GelMA microspheres, flow rates of both aqueous GelMA and oil solutions, and the viscoelastic properties of GelMA solutions at varying concentrations, were optimized. Since the oil solution (continuous phase) flow rates provide shear forces for the generation of GelMA microspheres, the flow rate of the oil phase was always set to be faster than the aqueous GelMA phase. Flow rates for the oil (continuous) phase and aqueous GelMA (dispersion) phase were optimized for target sizes varying from 35 to 250 μm [Fig. 2(a)]. Generation of microsphere sizes of 50, 100, and 150 μm was demonstrated using a wide range of GelMA concentrations (7–15%) [Fig. 2(b)] with low, medium, and high flow rate ratios [as indicated in Fig. 2(a)]. [GelMA:oil (μL/min) = low (45.725:75.68), medium (65.27:89.32), and high (72.67:93.76)]. Across the testing range, increasing the phase flow rate resulted in microspheres with larger diameters. The size difference between constructs formed under low flow conditions was determined to be statistically significant (One-way ANOVA, $P < 0.001$) than those formed under either medium or high flow rates for all the chosen solution concentrations. The data also suggest that despite changes in GelMA concentrations, microspheres of similar dimensions were achievable under the same flow conditions. GelMA concentrations of 3 and 5% were not able to form stable microspheres. For concentrations of 6, 7, and 8%, GelMA could flow easily throughout the device and form microspheres in a repeatable manner. However, GelMA concentration of 10% or more

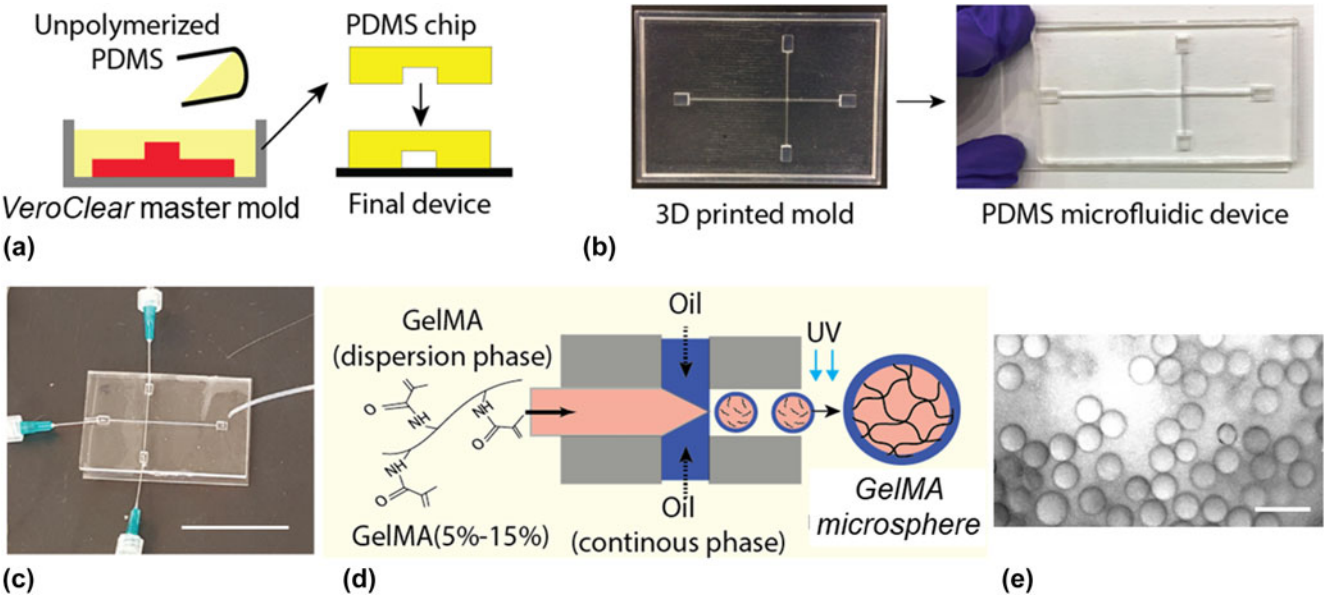

FIG. 1. Design and development of the microfluidic device for the generation of hydrogel microspheres. (a) Schematic showing PDMS casting using VeroClear negative mold (red), and PDMS chip plasma bonded with glass substrate to build a microfluidic device. (b) Picture of VeroClear mold (left) and the final PDMS device (right). (c) Integration of microfluidic device to pump setup. Note the use of Leur tapers to allow for uninterrupted flow between FEP tubing and 23G needles. Scale bar: 5 cm. (d) Schematic of process flow to generate GelMA microspheres. (e) Representative bright field image of GelMA microspheres with an average diameter of 35 μm (scale bar: 50 μm).

experienced rapid gelation at room temperature and would clog within the FEP tubing and the microfluidic channels, possibly due to greater viscosities within the channels. UV-exposure time as a function of GelMA concentration was also obtained [Fig. 2(c)].

2. Viscosity characterization

To investigate the mechanical properties of different GelMA solution, viscosity profiles were obtained. [Fig. 2(d)]. Solution viscosity of GelMA solutions with varying concentrations [3, 5, 6, 7, 8, 10, 12, and 15% (w/v)] was characterized at shear rates that correspond to three sections within the device: (1) FEP tubing, (2) syringe tip, and (3) T-junction (the site of microsphere generation). Shear rates experienced by GelMA solutions while flowing through the various sections of the setup were calculated and identified on the rheological profiles. This was done by modeling the aqueous GelMA phase as an incompressible Newtonian fluid flowing through a cylinder.[28,29] The maximum shear rate (obtained at the edge of the cylinder) was calculated by $\dot{\gamma} = 32Q/\pi D^2$, where Q represents the flow rate and D is the cross-sectional diameter. As the channels had a rectangular cross-section, the equivalent diameter was calculated by $D_{\text{rec}} = 2/\left(\frac{1}{a}+\frac{1}{b}\right)$, where a and b are the sides of the channel. GelMA solutions experience the highest shear rate, $\dot{\gamma}$ of 271.88 (1/s) at the outlet channels [0.150 × 4 mm, Fig. 2(d)(3)]; γ = 171.75 (1/s) at the 23G syringe tip [ID: 0.337 mm, Fig. 2(d)(2)]; and γ = 50.14 (1/s) inside the FEP tubing [ID: 0.508 mm, Fig. 2(d)(1)]. Based on experimental observations with various GelMA concentrations, viscosity values of solution concentrations between 6 and 8% (w/v) flow well within the channels and generate GelMA microspheres in a reliable manner.

As suggested by the previous work, increasing the concentration of the GelMA prepolymer phase was expected to yield hydrogels with different mechanical properties, such as storage and compressive moduli.[20] With the goal of achieving long-term structural stability of GelMA microspheres, we choose the highest concentration of GelMA that can be reliably flown through the device (8% w/v) without clogging the channels. Low UV cross-linking time is also desirable for high viability of cells during the encapsulation experiments. Since 8% showed the lowest UV cross-linking time as compared to 6–8% GelMA concentration range, 8% GelMA was chosen for work with cell-laden hydrogels.

Since hydrogels are characterized by high swelling rates, final microsphere sizes for 8% (w/v) GelMA were measured pre-and post-swelling for a period of 4 h [Fig. 2(e)]. GelMA microspheres were generated for a wide size range (diameters: 35–250 μm), and change in microsphere was measured at selected time points. Smaller microspheres show the highest percent increase in size as compared to larger sizes. For instance, microspheres with 50 μm initial diameter saw a 35% increase in this dimension, while 100 μm and 150 μm constructs expanded only about 16.5% and 8.6%, respectively. All

samples show saturation in swelling response after types showed full swelling after 3 h of incubation in DI water.

C. Cell-laden GelMA microspheres

Human Saos-2 cells were mixed in varying densities within a sterile solution of 8% GelMA. Process parameters were chosen to generate a target microsphere size of 100 μm, and cell-laden microspheres were generated using the process described throughout the methods section. Cell densities were varied from 10^5 to 10^6 to determine the maximum number of cells that can be encapsulated within the microspheres while maintaining high viability. The results identified a maximum density of 6.0×10^5 cells/mL as the ideal cell density for encapsulation experiments [Fig. 3(a)] Above this cell density, the viability of cells drop significantly. The viability within the constructs only decreased about 20% for 6.0×10^5 cells/mL for a period of 3 weeks ($n = 10$). By contrast, higher cell densities showed a 65–90% drop in cellular viability for a period of 3 weeks ($n = 10$). As a result, the optimized cell density of 6.0×10^5 cells/mL was used to generate cell-laden microspheres of varying sizes [Fig. 3(b)]. A Pearson's correlation test was performed on these data and it was found that there is a significant correlation between the microsphere mean diameter and the number of cells encapsulated, thereby allowing control over the number of cells per microsphere.

Representative images of cell-laden GelMA microspheres (100 μm) incubated both in water and perfluorodecalin oil show the sphere boundary and the

	Flow Rate Aqueous Phase (μL/min)	Flow Rate Oil Phase (μL/min)	Mean Microsphere diameter (μm)
	38.72	42.57	35 ± 0.75
Low →	*45.73*	*75.68*	*50 ± 0.73*
	52.32	80.24	80 ± 0.50
Medium →	*65.27*	*89.32*	*100 ± 0.88*
High →	*72.67*	*93.76*	*150 ± 0.79*
	85.78	96.27	200 ± 0.99
	90.25	108.76	250 ± 0.35

(a)

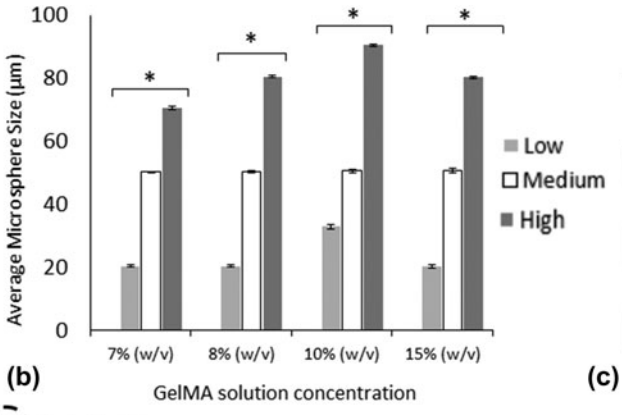

(b)

GelMA (% w/v)	UV time (sec)
5	250
7	170
8	***115***
10	60
15	45

(c)

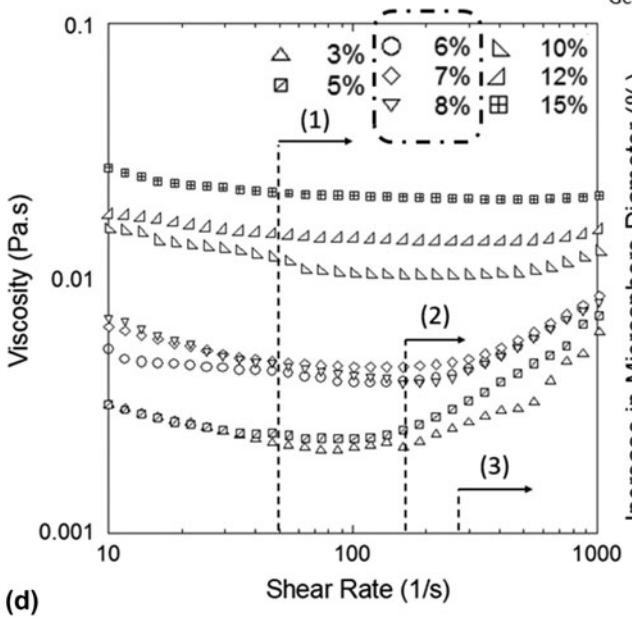

(d)

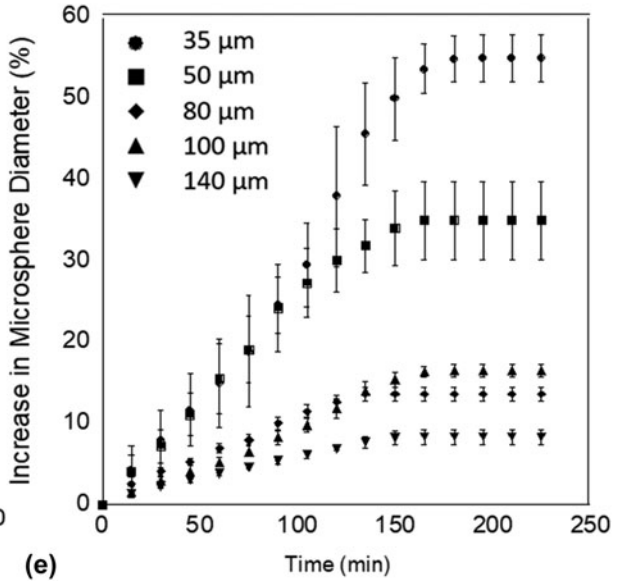

(e)

FIG. 2. Material characterization and optimization of process conditions. (a) Table showing the relationship between flow rates of oil and 8% GelMA phases, and final microsphere sizes. (b) Range of microsphere sizes obtained at low, medium, and high flow rate of GelMA and oil phases, as indicated in (a) using GelMA solutions of four different concentrations. One-way ANOVA, $n = 10$, $P < 0.001$ (*) (c) table showing the UV exposure time needed to crosslink microspheres of varying GelMA concentrations. (d) Solution viscosity of GelMA solutions with varying concentrations [3, 5, 6, 7, 8, 10, 12, and 15% (w/v)] characterized at different shear rates that correspond to three sections within the device, (1) FEP tubing, (2) syringe tip, and (3) T-junction (the site of microsphere generation). (e) Swelling profiles of GelMA microspheres of varying initial diameters over a period of 4 h.

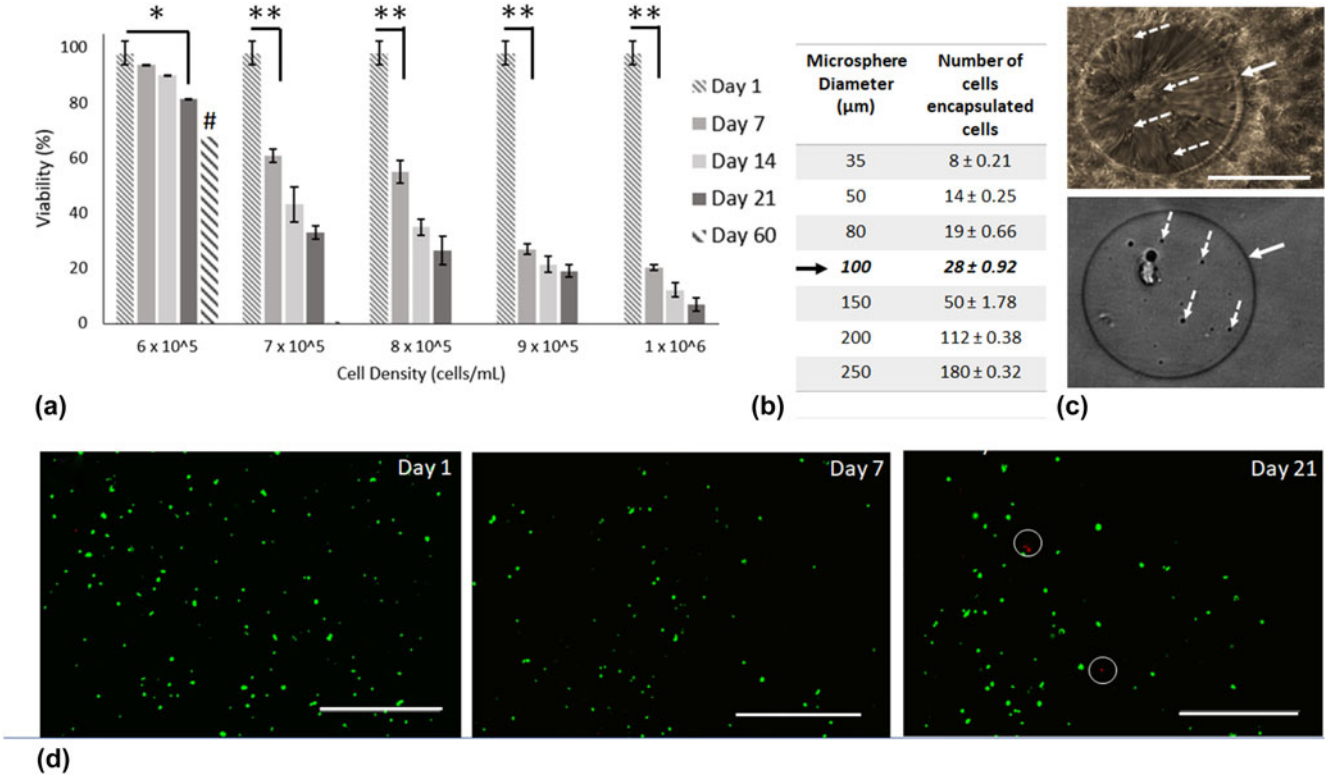

Microsphere Diameter (μm)	Number of cells encapsulated cells
35	8 ± 0.21
50	14 ± 0.25
80	19 ± 0.66
100	**28 ± 0.92**
150	50 ± 1.78
200	112 ± 0.38
250	180 ± 0.32

FIG. 3. Characterization of cell-laden hydrogel microspheres. (a) Percent viability of cells as a function of density and time. For 6×10^6 cells/mL viabilities of 93.75%, 90.125%, 81.25%, and 68.75% on days 7, 14, 21, and 60, respectively. One-way ANOVA, $n = 10$, [$P < 0.05$ (*), $P < 0.001$ (**)] (except on day 60; $n = 1$, #), (b) table relating microsphere size, and the number of encapsulated human Saos-2 cells with a solution density of 6×10^5 cell/mL. (c) Bright field images (40×; scale bar: 100 μm) show a single GelMA microsphere in 1×-DPBS (top) and perfluorodecalin oil (bottom) (Solid arrow—microsphere boundary; dashed arrow—encapsulated cells). (d) Fluorescent images (10×; scale bar: 100 μm) showing live (green) and dead (red–white circle on day 21) in cell-laden GelMA microspheres on day 1, day 7, and day 21.

encapsulated cells inside the microspheres. Representative live/dead staining images for 100 μm with a cell density of 6.0×10^5 cells/mL show good viability for earlier time-points, and only a few dead cells [red, Fig. 3(d) white circles].

This method can be potentially used to generate cell-laden microspheres for a wide variety of applications. However, it should be noted that additional factors such as cell size, sensitivity to shear stress, and cell density would be expected to play a role in cell viability. Although UV light was used as a cross-linking mechanism, other mechanism and hydrogels, such as alginate hydrogels and calcium ion-based cross-linking methods can also be used.[11,30]

IV. CONCLUSION

A 3D printing-based method to design and develop a microfluidic device capable of generating cell-laden microspheres is presented. Key process parameters such as viscosity of hydrogel solutions, microsphere sizes, swelling properties, and cell densities were optimized. This work demonstrates the fabrication of microfluidic devices in a simple and inexpensive manner without the use of traditional cleanroom facilities, or specialized equipment, often used in traditional microfluidics. The use of 3D printing lowers the barrier to entry in microfluidics and related application areas in biomedical engineering.

AUTHOR CONTRIBUTION

S.S. and P.S. conceived and designed the experiments; S.S. and S.M. carried out microfluidic work; S.S., S.W.S., and R.R. performed cell studies; R.R. and S.M. synthesized GelMA macromer.

ACKNOWLEDGMENT

This work was partially supported by the Nappi Family Research Award and CMMI 1547095 (National Science Foundation).

REFERENCES

1. X. Zhao, S. Liu, L. Yildirimer, H. Zhao, R. Ding, H. Wang, W. Cui, and D. Weitz: Injectable stem cell-laden photocrosslinkable microspheres fabricated using microfluidics for rapid generation of osteogenic tissue constructs. *Adv. Funct. Mater.* **26**, 2809 (2016).

2. V. van Duinen, S.J. Trietsch, J. Joore, P. Vulto, and T. Hankemeier: Microfluidic 3D cell culture: From tools to tissue models. *Curr. Opin. Biotechnol.* **35**, 118 (2015).
3. A. Kang, J. Park, J. Ju, G.S. Jeong, and S-H. Lee: Cell encapsulation via microtechnologies. *Biomaterials* **35**, 2651 (2014).
4. Y-C. Lu, W. Song, D. An, B.J. Kim, R. Schwartz, M. Wu, and M. Ma: Designing compartmentalized hydrogel microparticles for cell encapsulation and scalable 3D cell culture. *J. Mater. Chem. B* **3**, 353 (2015).
5. K. Yue, G. Trujillo-de Santiago, M.M. Alvarez, A. Tamayol, N. Annabi, and A. Khademhosseini: Synthesis, properties, and biomedical applications of gelatin methacryloyl (GelMA) hydrogels. *Biomaterials* **73**, 254 (2015).
6. W.H. Tan and S. Takeuchi: Monodisperse alginate hydrogel microbeads for cell encapsulation. *Adv. Mater.* **19**, 2696 (2007).
7. D. Dupin, S. Fujii, S.P. Armes, P. Reeve, and S.M. Baxter: Efficient synthesis of sterically stabilized pH-responsive microgels of controllable particle diameter by emulsion polymerization. *Langmuir* **22**, 3381 (2006).
8. M. Antonietti, W. Bremser, D. Mueschenborn, C. Rosenauer, B. Schupp, and M. Schmidt: Synthesis and size control of polystyrene latices via polymerization in microemulsion. *Macromolecules* **24**, 6636 (1991).
9. A. Kumachev, J. Greener, E. Tumarkin, E. Eiser, P.W. Zandstra, and E. Kumacheva: High-throughput generation of hydrogel microbeads with varying elasticity for cell encapsulation. *Biomaterials* **32**, 1477 (2011).
10. J.W. Kim, A.S. Utada, A. Fernández-Nieves, Z. Hu, and D.A. Weitz: Fabrication of monodisperse gel shells and functional microgels in microfluidic devices. *Angew. Chem.* **119**, 1851 (2007).
11. V.L. Workman, S.B. Dunnett, P. Kille, and D. Palmer: Microfluidic chip-based synthesis of alginate microspheres for encapsulation of immortalized human cells. *Biomicrofluidics* **1**, 014105 (2007).
12. T. Li, L. Zhao, W. Liu, J. Xu, and J. Wang: Simple and reusable off-the-shelf microfluidic devices for the versatile generation of droplets. *Lab Chip* **16**, 4718 (2016).
13. A.K. Au, W. Huynh, L.F. Horowitz, and A. Folch: 3D-printed microfluidics. *Angew. Chem., Int. Ed.* **55**, 3862 (2016).
14. N. Bhattacharjee, A. Urrios, S. Kang, and A. Folch: The upcoming 3D-printing revolution in microfluidics. *Lab Chip* **16**, 1720 (2016).
15. P.J. Kitson, M.H. Rosnes, V. Sans, V. Dragone, and L. Cronin: Configurable 3D-printed millifluidic and microfluidic 'lab on a chip'reactionware devices. *Lab Chip* **12**, 3267 (2012).
16. S. Waheed, J.M. Cabot, N.P. Macdonald, T. Lewis, R.M. Guijt, B. Paull, and M.C. Breadmore: 3D printed microfluidic devices: Enablers and barriers. *Lab Chip* **16**, 1993 (2016).
17. L.D. Albrecht, S.W. Sawyer, and P. Soman: Developing 3D scaffolds in the field of tissue engineering to treat complex bone defects. *3D Print. Addit. Manuf.* **3**, 106 (2016).
18. K.M. Ogden, C. Aslan, N. Ordway, D. Diallo, G. Tillapaugh-Fay, and P. Soman: Factors affecting dimensional accuracy of 3-D printed anatomical structures derived from CT data. *J. Digit. Imag.* **28**, 654 (2015).
19. L. Yang, S.V. Shridhar, M. Gerwitz, and P. Soman: An in vitro vascular chip using 3D printing-enabled hydrogel casting. *Biofabrication* **8**, 035015 (2016).
20. S. Sawyer, M. Oest, B. Margulies, and P. Soman: Behavior of encapsulated saos-2 cells within gelatin methacrylate hydrogels. *J. Tissue Sci. Eng.* **7**, 2 (2016).
21. Y.X. Chen, S. Yang, J. Yan, M-H. Hsieh, L. Weng, J.L. Ouderkirk, M. Krendel, and P. Soman: A novel suspended hydrogel membrane platform for cell culture. *J. Nanotechnol. Eng. Med.* **6**, 021002 (2015).
22. F. Tamimi, P. Comeau, D. Le Nihouannen, Y. Zhang, D. Bassett, S. Khalili, U. Gbureck, S. Tran, S. Komarova, and J. Barralet: Perfluorodecalin and bone regeneration. *Eur. Cell. Mater.* **25**, 22 (2013).
23. V. Chokkalingam, B. Weidenhof, M. Krämer, W.F. Maier, S. Herminghaus, and R. Seemann: Optimized droplet-based microfluidics scheme for sol–gel reactions. *Lab Chip* **10**, 1700 (2010).
24. D. Kumar, I. Gerges, M. Tamplenizza, C. Lenardi, N.R. Forsyth, and Y. Liu: Three-dimensional hypoxic culture of human mesenchymal stem cells encapsulated in a photocurable, biodegradable polymer hydrogel: A potential injectable cellular product for nucleus pulposus regeneration. *Acta Biomater.* **10**, 3463 (2014).
25. C. Chung, J. Mesa, M.A. Randolph, M. Yaremchuk, and J.A. Burdick: Influence of gel properties on neocartilage formation by auricular chondrocytes photoencapsulated in hyaluronic acid networks. *J. Biomed. Mater. Res., Part A* **77**, 518 (2006).
26. Y.X. Chen, B. Cain, and P. Soman: Gelatin methacrylate-alginate hydrogel with tunable viscoelastic properties. *AIMS Mater. Sci.* **4**, 363 (2017).
27. S.W. Sawyer, P. Dong, S. Venn, A. Ramos, D. Quinn, J.A. Horton, and P. Soman: Conductive gelatin methacrylate-poly(aniline) hydrogel for cell encapsulation. *Biomed. Phys. Eng. Express* **4**, 015005 (2017).
28. F.M. White: *Fluid Mechanics* (WCB Ed McGraw-Hill, Boston, 1999).
29. R.G. Larson: *The Structure and Rheology of Complex Fluids* (Oxford University Press, New York, 1999).
30. P. Agarwal, S. Zhao, P. Bielecki, W. Rao, J.K. Choi, Y. Zhao, J. Yu, W. Zhang, and X. He: One-step microfluidic generation of pre-hatching embryo-like core–shell microcapsules for miniaturized 3D culture of pluripotent stem cells. *Lab Chip* **13**, 4525 (2013).